Brief review of recent research on blue phase liquid crystal materials and devices

Zhi-gang Zheng (郑致刚)[1,2], Wei Hu (胡 伟)[1], Ge Zhu (诸 戈)[1], Mu Sun (孙 牧)[3], Dong Shen (沈 冬)[2], and Yan-qing Lu (陆延青)[1*]

[1] *National Laboratory of Solid State Microstructures and College of Engineering and Applied Sciences, Nanjing University, Nanjing 210093, China*

[2] *Department of Physics, East China University of Science and Technology, Shanghai 200237, China*

[3] *Chemical Defence Institute, Beijing 102205, China*

[*] *Corresponding author: yqlu@nju.edu.cn*

Received November 1, 2012; accepted November 16, 2012; posted online January 6, 2013

Both polymer stabilization and bent-shaped molecule doping strategies are utilized to widen the blue phase range of liquid crystals. The molecular structures of compositions are optimized for high thermo-optical and electro-optical performances. A low temperature applicable blue phase liquid crystal with suppressed hysteresis is achieved. The bistability of one blue phase liquid crystal is investigated. Based on these materials, fast tunable devices such as gratings with polarization insensitivity are designed and fabricated. The materials and device designs demonstrated here are suitable in wide applications requiring fast response time.

OCIS codes: 160.3710, 050.1950, 160.4670.
doi: 10.3788/COL201311.011601.

It is well known that the nematic, smectic, and cholesteric are three typical phases of the conventional liquid crystals (LCs). The blue phase (BP) is also a special LC phase which normally exists in the materials with large twisted power. When such material is cooled down, many colorful platelet textures can be found in a very narrow temperature range (1–2 K) between the isotropy and chiral nematic phases, that is the BP[1]. Many theoretical analysis and experimental phenomenon have revealed that LC alignment in BP is complex and exotic. Not like the single twisted assembling in cholesteric phase, LC molecules are double twisted assembled in BP. The two twisted axes are crossed with each other and form the double twisted cylinders (DTCs). These DTCs can either exist in disordered distribution, exhibiting a fog-like texture (BP III), or self-assemble into three-dimensional (3D) crystals, showing colorful platelet textures (BP I and BP II) due to the selective Bragg reflections[2,3]. The unique structure of BP LC endows it with some interesting characteristics, such as optical isotropy at voltage off state, fast response time down to submillisecond, which are much benefit for the next generation of display and photonic devices[4−10]. Although BP LC was found a century ago, it was failed to be applied realistically for quite a long time due to its instinct problems, especially its narrow temperature range.

Many efforts have been made to overcome this shortage. Some great improvements have been achieved during the last decade. The first promising wide temperature range BP was demonstrated by Kikuchi *et al.*[11]. They uniformly mixed acrylate based monomers into chiral nematic LCs, and then exposed the mixture under UV at BP state to polymerize the monomers. Finally, the BP was stabilized by polymer network, and the BP range was extended to over 60 °C. This is the so called polymer stabilized BP (PSBP). The mechanism of PSBP is that the polymer forms a stable 3D framework and stabilizes the defects in the frustration BP system. After this strategy was established, especially after Samsung exhibited the first BP LC display (LCD) at SID Display Week in Los Angeles, in 2008, more and more attentions had been attracted by the promising materials. Wu's group[12] has made great contributions to the improvement of PSBP materials, e.g., they reported a kind of PSBP material with a large Kerr constant of 13.7 nm/V^2, which is 3∼10 times higher than the conventional BPLCs. A kind of high dielectric constant ($\Delta\varepsilon$ ∼94) nematic LCs was selected to prepare such PSBP, and low drive voltage (RMS) of 48 V, high contrast ratio of 1000:1 for the PSBP was obtained. And they also pointed out that the drive voltage could even reduce to less than 10 V, if using the protrusion electrode cell[12,13]. This is undoubtedly a major breakthrough for the applications of PSBP on thin film transistor (TFT)-LCD. In addition, the PSBP with negative Kerr effect (–0.16 nm/V^2) was also reported by this group[14]. Although it is smaller compared with typical positive PSBP, such negative PSBP can be driven with conventional planar electrode and is useful for controlling the viewing angle of LCD as the C-plate. Wittig *et al.* also reported a BPLC host with huge $\Delta\varepsilon$ of larger than 190[15]. So the Kerr constant was supposed to be improved in further. These excellent works have well solved some of the bottleneck problems of BP LCs and obtained better electro-optical behaviors. Thus, from the current development of BP LCs materials, PSBP is indeed a mainstream technology to be applied in practice. However, the electro-optical hysteresis is still a major problem which arises out of the polymer networks. In addition, critical temperature controls are necessary as a result of the narrow BP range of pre-UV mixtures. Such rigorous process condition brings the inconvenience for the production. Considering to that, other methods to obtain wide temperature range BP LCs were also proposed recently.

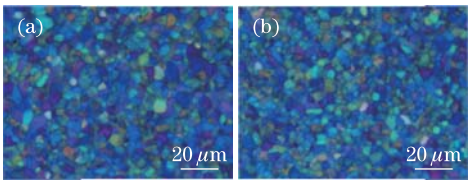

Fig. 1. BP textures at (a) room temperature (20 °C) and (b) –35 °C.

Some researchers tried to extend BP range via chemical synthesis, for instance, Coles *et al.* connected two mesogens with long flexible hydrocarbon chain by synthetic methodologies and obtained a series of bimesogen based LCs[16]. Such kinds of materials have large elastic constant and flexoelectricity, which facilitates the decreasing of free energy in BP system, and the BP range is widened to 44 °C correspondingly. Yoshizawa *et al.* synthesized some T-shaped and binaphthyl based molecules, and obtained two kinds of materials with the BP range of 13 and 29 °C, respectively[17,18]. The wide temperature ranges mainly depend on the special configurations of the two molecules. He *et al.* designed a novel fluoro-substituted H-bonded LC, which could form a broad temperature range of BP II through H-bond self-assembly[19]. The BP range of such materials could reach ∼ 23 °C. Japanese researchers claimed that the BP range can be widened to 5 °C by adding a small amount of aurum nanoparticles in BP system, because of the decreasing of the interfacial energy between DTCs and defects induced by the large specific surface area of nanomaterials[20]. Besides, an ingenious hysterisis-free BP with a temperature range of 15.6 °C was obtained by doping a very small amount of hydrophobic surface-treated ZnS nanoparticles into the conventional BP systems[21]. The authors demonstrated the good electro-optical performances and large Kerr constant of such materials. Although these materials are less effective compared to PSBP and still have a long-distance away from real application, they suggest some possible strategies for wide blue phase range.

Researchers in our group have developed a low-temperature-applicable and wide temperature range PSBP[22]. A series of acrylate based molecules with similar calamitic structure and two photopolymerizable alkenyl end-groups were utilized as the LCs. Two types of monomers with different lengths of end-group, $PTPTP_3$ and $PTPTP_6$, were selected and mixed with 2-Ethylhexyl acrylate to increase the cross-linkage of polymer network. The structure of $PTPTP_n$ series is similar to the bistolane LCs previously studied by Wu *et al.*[23,24], For stability improvement, the UV-unstable triple bond in the bistolane is replaced by the more stable ester group, and the end group is replaced by the photopolymerizable alkenyl chain. The similar molecular structure of $PTPTP_n$ to conventional LCs makes a good miscibility and reduces the negative effect of monomers on BP arrangement. The BP range is extended to more than 70 °C, and what's more, the BP material works well at low temperature down to –35 °C. Figures 1(a) and (b) reveal the PSBP texture at room temperature and –35 °C, respectively. However, objectively speaking, the clearing point of the PSBP herein is 35 °C, which is insufficient for practice applications and need to be further improved. Utilizing high clearing point LCs as host will be a direct and effective way for raising the clearing point, and increasing the cross linking density of polymer network at the same time to keep the BP structure at low temperature. However, higher cross linking density will lead to larger hysteresis effect, so there is a tradeoff between them. A uniform-electric-field-driven method was proposed and used for the Kerr constant measurement. The voltage dependent birefringence of PSBP was tested through the conventional Senarmont's method. However, the normal of sample is not parallel to the wave vector, but in certain oblique angle θ, thus Kerr constant $K(\theta)$ can be calculated and $K \sim \theta$ equation is obtained by fitting the datum. The Kerr constant of PSBP is defined as the value of K when θ is 90°. This method avoids the effect of non-uniformity of electric field in in-plane-switching cell and presents the inner properties of materials more directly. The measured Kerr constant of the material is 2.195 nm/V^2 at room temperature, while it is a slightly decrease to 2.077 nm/V^2 at –35 °C, which is opposite to the analysis by Rao *et al.*[12,13]. In their experiments, Kerr constant increases with the decreasing of temperature. We consider the reason for this difference is due to the polymer network. In our PSBP system, high cross linking density polymer network of $PTPTP_n$ is formed and the glass transition temperature of polymer raises which leads to the decreasing of flexibility and increasing of toughness at lower temperature[25]. Therefore the anchoring effect increases and leads to the raise of saturated electric field (E_S). From the other aspect, the increased viscosity of LCs also brings to a high E_S. Due to the above two reasons, E_S in high cross linking density system is much increased. The increasing rate of PSBP birefringence (Δn_s) is not slower than that of E_S; in addition, Kerr constant is inversely proportional to E_S^2, but proportional to Δn_s[26], therefore the Kerr constant of PSBP at low temperature is smaller. Although the Kerr constant of such PSBP is lower than reported ones, this material shows good properties at low temperature, so it might be promising in low-temperature displays or other photonic applications. The testing of electro-optical properties show that the saturation voltage increases and the hysteresis enhances as the increasing of polymer concentration. Such material shows good electro-optical behavior even at low temperature. The rise and decay times, tested at room temperature with the signal frequency of 1 kHz, reach 391 and 789 μs, both down to submillisecond respectively.

Recently, bistable BP LCs system has been discovered. Wang *et al.* reported the bistable states of BP I and BP II that found in BP LCs system, and their phase transition behaviors were also studied[27]. The PSBP bistability was also found[28]. Unlike conventional PSBP, which went from PSBP directly to field-induced vertical alignment (VA) when driven by saturated electric field, an intermediate chiral nematic phase was observed between the above two states when the applied field was increased slowly to the saturation. Similarly, when the field is declined slowly, the sample shows a stable chiral nematic phase as well, even though the field is totally removed. In the other case, when the field is applied and removed suddenly, reversible direct transitions between BP and VA can be realized. Therefore two stable phases,

blue phase and chiral nematic state, are obtained and the bistable can modulated with different operation procedures. The tested electro-optical performance is given in Fig. 2(a) and the electric field induced phase transition is schematically shown in Fig. 2(b). We ascribe the bistablity to the weaker elastic force of polymer network caused by the lower crosslinking density. We suppose the bistable phenomenon may widely exist in PSBP system, however, in traditional PSBPs, the polymer elastic force is so strong that the applied electric field force is difficult to destroy the BP. If the polymer elastic force is deliberated decreased through molecular composition tailorings, the bistability may appear.

Besides researches on PSBP, new strategies towards wide BP range by doping with some amount of achiral bent-shaped molecules were also investigated[29]. Less than 10 wt.% oxadiazole based bent-shaped molecules were doped into a chiral nematic system, and then a 29 °C-temperature-range-BP was achieved, with textures as shown in Fig. 3(a). The mechanisms of the wide BP range were analyzed combined with theoretical calculations. As schemed in Fig. 3(b), we consider the coupling between the chirality of chiral dopant and biaxiality of bent-shaped molecules enhances the double twisted arrangement of BP; moreover, the existence of bent-shaped molecules can decrease the interfacial energy between DTCs and defects, and leads to the reduction of free energy. We also found that molecular properties, such as dipole moment, LC phase and melting point of the bent-shaped dopant, affect the BP range as well. The influences of molecular structure on BP range were studied[30,31]. The bent-shaped molecules with longer terminal chains decrease the interfacial energy between DTCs and defects more efficiently, and facilitate the stabilization of BP. Extending the rigid body of the bent-shaped molecules will increase the biaxiality of the molecules, and facilitate the stabilization of BPs as well. Through doping with bent-shaped molecules with allylic

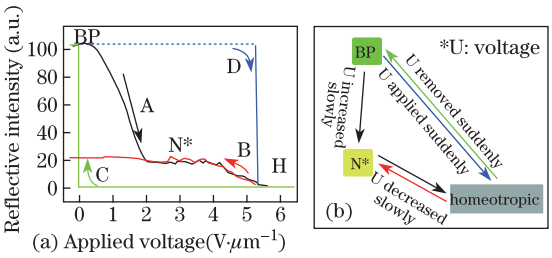

Fig. 2. (a) Tested electro-optical curves of bistable PSBP and (b) schematic electric field induced phase transition. 'A', 'B', 'C', 'D' labeled in (a) refer to four operational steps of increased (A), or decreased (B) the voltage slowly, and appleed (D) or removed (C) the voltage with a sudden. 'H' refers to homeotropic alignment.

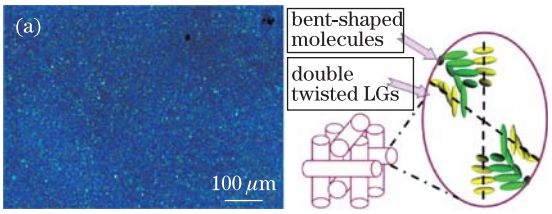

Fig. 3. (a) Texture of bent-shaped-molecule-induced BP and (b) model of DTC induced by bent-shaped molecule.

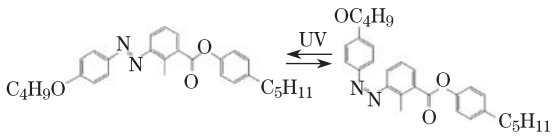

Fig. 4. Photoisomerization of azobenzene bent-shaped molecule.

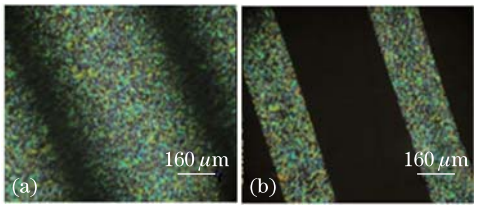

Fig. 5. Stripes recorded in azobenzene doped BP system (a) before and (b) after exposure.

end groups, the authors reported a 6 K-BP-range[32]. After UV irradiation, the BP range was further extended to 10.2 K. We assumed the evident extension to the longer rigid body of molecules caused by photoreaction.

A kind of azobenzene based bent-shaped molecule was synthesized. The molecule can change it shape by photoisomerization under 365-nm UV[33]. As shown in Fig. 4, the stable configuration of this molecule is bent (or trans-configuration), while turns to linear shape (or cis-configuration) rapidly after UV exposure due to the trans-cis photo-isomerization of azo-group. In this case, BP disappears and is instead by chiral nematic phase. When the material is stayed at dark for a while, the cis-trans isomerization leads to the emergence of BP again. This makes the light-driven BP possible. Some stripe patterns were recorded in such materials by exposing through a photomask. Figure 5 shows the stripe patterns. In the initiate, the sample was BP state (Fig. 5(a)), after 1-min-exposure, the exposed area transited to isotropic state (Fig. 5(b)). The edge between BP and isotropic area was very clear, which indicates a good locality for the material to form the fine micro-patterns.

As mentioned above, the fast response of BP permits the fabrication of fast switching elements. Herein we take LC gratings as an example, which could be utilized as tunable passive components such as filters, switches, and modulators, etc.[34]. Response/switching time is a key parameter that determines the performance of these components. For common nematic LCs, it is usually limited to the level of tens of milliseconds[35,36]. For fast tuning purpose, several special materials like ferroelectric LCs[34] and dual frequency LCs[37] have been raised to shorten the response time. BP LCs also show a possibility of submilisecond response, and grating designs based on this material are also proposed[38].

In our experiment, the PSBP shown in Fig. 1 is utilized. Through electrode configuration design, both 1D and 2D gratings could be accomplished[39]. In Fig. 6(a), a cell with striped electrode on one side and a planar electrode on the other side was presented. An achromatic light beam is normally incident to the cell. At off state, LC refractive indices in the two alternating regions are uniform as n_{iso}, therefore no diffraction could be observed. When an AC signal is applied (on state, as shown in Fig. 6(b)), LC refractive index would change to n_o in

the striped electrode covered regions, while that in the electrode gap regions remains approximately unchanged. As a result, the incident light is diffracted.

2D gratings are fabricated by assembling a cell with striped electrodes on both substrates orthogonally (Fig. 6(c)). The electrodes are employed to generate a vertical electric field with lateral periodic field intensity distribution. According to Kerr effect, refractive index change occurs cyclically on each electrodes covered region, but does not occur at gap domains. That indicates alternating refractive indices of ordinary and isotropic are exhibited laterally, despite of polarization of incident light, providing a polarization independent phase grating profile.

The electro-optical properties of a 1D PSBP LC grating were tested. The two curves in Fig. 7(a) show ratios of the light power collected from 0th and 1st orders divided by total transmittance at off state respectively. As expected, no threshold voltage is observed as the mechanism of field induced birefringence. And the intensity of 0th order and 1st order mirrors each other varies as a function of applied voltage. The phase retardation has not reached one π so that the intensity of 0th or 1st order does not exhibit an extremum. However, the diffraction efficiency of 1st order (defined as the ratio between the intensity of 1st order and total transmitted) has still reached up to 38.7% at 55 V, comparable to that reported with a phase retardation of π (40% at 160 V)[37]. This indicates the diffraction intensity here is very close to a maximum. The insets in Fig. 7(a) provide some photos of diffraction patterns. The patterns follow the curves very well and directly prove the tunability of the gratings. At voltage-off state, weak diffraction patterns could be observed due to the striped electrodes. Two comparatively strong dots appear, the reason of which is supposed to be the orientation of LC molecules by the relief boundaries of electrodes, forming a grating with half period of original striped electrodes.

The polarization direction of incident light beams was changed and then transmittance curves of 1st order under each circumstance are recorded. In Fig. 7(b) three typical curves are presented. These curves are in good accordance with each other that obviously reveals the grating's good polarization independency under normal incidence. The insets show the patterns taken at 40 V, their highly similarity is coincident with the above discussions.

The switching on/off time, defined as 10% to 90% in transmittance and reverse, of the presented grating is also tested. Measured values are 380 and 860 μs respectively. Both data are in submillisecond range. The

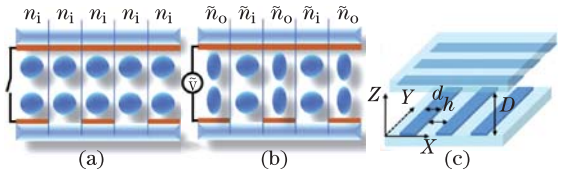

Fig. 6. Schematic diagrams of the effective optical index-ellipsoids of PSBPLC in 1D grating structure at voltage (a) off and (b) on state respectively; (c) structure of 2D grating with electrode directions on two substrates orthogonal.

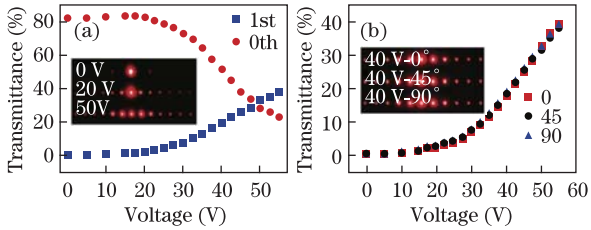

Fig. 7. (Color online) Diffraction patterns (insets) and efficiencies of (a) 0th and 1st orders; (b) 1st orders under different polarized incident lights.

fast switching time permits the proposed gratings being applied to a wide field of tunable optical elements and devices, such as optical interconnects, beam steering devices and spatial light modulators.

In conclusion, we review several recently developed strategies for BP range extending, present a low temperature applicable BP LC, study the bistability of BP LC and investigate an optical writable BP material. Based on a PSBP material, a fast tunable grating is designed and fabricated. The materials and device design demonstrated here show some new insights for novel high performance BP LC materials and corresponding components.

The authors thank Prof. Shin-Tson Wu for his continuous encouragement and guidance. This work was supported by the National "973" Program of China (Nos. 2011CBA00200 and 2012CB921803), the National Natural Science Foundation of China (Nos. 61225026 and 61108065), and the China Postdoctoral Science Foundation (No. 20110491370). The authors also thank the supports from IVO Co.

References

1. T. Kato, *Liquid Crystalline Functional Assemblies and Their Supramolecular Structures* (Springer, New York, 2008).
2. H. S. Kitzerow, Chem. Phys. Chem. **7,** 63 (2006).
3. D. C. Wright and N. D. Mermin, Rev. Mod. Phys. **61,** 385 (1989).
4. J. Yan and S. T. Wu, Opt. Mater. Express **1,** 1527 (2011).
5. M. Z. Jiao, Y. Li, and S. T. Wu, Appl. Phys. Lett. **96,** 011102 (2010).
6. F. Zhou, J. P. Cui, Q. H. Wang, D. H. Li, and D. Wu, J. Display Technol. **7,** 170 (2011).
7. J. P. Cui, F. Zhou, Q. H. Wang, D. Wu, and D. H. Li, J. Display Technol. **7,** 398 (2011).
8. J. Yan, L. H. Rao, M. Z. Jiao, Y. Li, H. C. Cheng, and S. T. Wu, J. Mater. Chem. **21,** 7870 (2011).
9. Y. Li and S. T. Wu, Opt. Express **19,** 8045 (2011).
10. Y. H. Lin, H. S. Chen, H. C. Lin, Y. S. Tsou, H. K. Hsu, and W. Y. Li, Appl. Phys. Lett. **96,** 113505 (2010).
11. H. Kikuchi, M. Yokota, Y. Hisakado, H. Yang, and T. Kajiyama, Nat. Mater. **1,** 64 (2002).
12. L. Rao, J. Yan, S. T. Wu, S. Yamamoto, and Y. Haseba, Appl. Phys. Lett. **98,** 081109 (2011).
13. L. Rao, J. Yan, and S. T. Wu, J. Soc. Inf. Disp. **18,** 954 (2010).
14. Y. Li, Y. Chen, J. Yan, Y. Liu, J. Cui, Q. Wang, and S. T. Wu, Opt. Mater. Express **2,** 1135 (2012).

15. M. Wittig, N. Tanaka, D. Wilkes, M. Bremer, D. Pauluth, J. Canisius, A. Yeh, R. Yan, K. Skjonnemand, and M. Klasen-Memmer, SID Int. Symp. Digest Tech. Papers **43,** 25 (2012).
16. H. J. Coles and M. N. Pivnenko, Nature **436,** 997 (2005).
17. A. Yoshizawa, Y. Kogawa, K. Kobayashi, Y. Takanishi, and J. Yamamoto, J. Mater. Chem. **19,** 5759 (2009).
18. A. Yoshizawa, M. Sato, and J. Rokunohe, J. Mater. Chem. **15,** 3285 (2005).
19. W. L. He, G. H. Pan, Z. Yang, D. Y. Zhao, G. G. Niu, W. Huang, X. T. Yuan, J. B. Guo, H. Cao, and H. Yang, Adv. Mater. **21,** 2050 (2009).
20. H. Yoshida, Y. Tanaka, K. Kawamoto, H. Kubo, T. Tsuda, A. Fujii, S. Kuwabata, H. Kikuchi, and M. Ozaki, Appl. Phys. Express **2,** 1577 (2009).
21. L. Wang, W. L. He, X. Xiao, F. U. Meng, Y. Zhang, P. Y. Yang, L. P. Wang, J. M. Xiao, H. Yang, and Y. F. Lu, Small **8,** 2189 (2012).
22. Z. G. Zheng, H. F. Wang, G. Zhu, X. W. Lin, J. N. Li, W. Hu, H. Q. Cui, D. Shen, and Y. Q. Lu, J. Soc. Inf. Disp. **20,** 326 (2012).
23. S. T. Wu, C. S. Hsu, and K. F. Shyu, Appl. Phys. Lett. **74,** 344 (1999).
24. S. T. Wu, C. S. Hsu, Y. Y. Chuang, and H. B. Cheng, Jpn. J. Appl. Phys. **39,** L38 (2000).
25. M. Rubinstein and R. H. Colby, *Polymer Physics* (Oxford University Press, Oxford, 2003).
26. J. Yan, H. C. Cheng, S. Gauza, Y. Li, M. Jiao, L. Rao, and S. T. Wu, Appl. Phys. Lett. **96,** 071105 (2010).
27. C. T. Wang, H. Y. Lin, H. H. Cheng, and T. H. Lin, Appl. Phys. Lett. **96,** 041106 (2010).
28. Z. G. Zheng, D. Zhang, X. W. Lin, G. Zhu, W. Hu, D. Shen, and Y. Q. Lu, Opt. Mater. Express **2,** 1353 (2012).
29. Z. G. Zheng, D. Shen, and P. Huang, New J. Phys. **12,** 113018 (2010).
30. H. F. Wang, Z. G. Zheng, and D. Shen, Liq. Cryst. **39,** 99 (2012).
31. Z. G. Zheng, D. Shen, and P. Huang, New J. Phys. **13,** 063037 (2010).
32. G. Zhu, X. W. Lin, W. Hu, Z. G. Zheng, H. F. Wang, H. Q. Cui, D. Shen, and Y. Q. Lu, Opt. Mater. Express **1,** 1478 (2011).
33. Y. Wen, Z. G. Zheng, H. F. Wang, and D. Shen, Liq. Cryst. **39,** 509 (2012).
34. A. K. Srivastava, E. P. Pozhidaev, V. G. Chigrinov, and R. Manohar, Appl. Phys. Lett. **99,** 201106 (2011).
35. W. Hu, A. Srivastava, F. Xu, J. T. Sun, X. W. Lin, H. Q. Cui, V. Chigrinov, and Y. Q. Lu, Opt. Express **20,** 5384 (2012).
36. W. Hu, A. K. Srivastava, X. W. Lin, X. Liang, Z. J. Wu, J. T. Sun, G. Zhu, V. Chigrinov, and Y. Q. Lu, Appl. Phys. Lett. **100,** 111116 (2012).
37. X. W. Lin, W. Hu, X. K. Hu, X. Liang, Y. Chen, H. Q. Cui, G. Zhu, J. N. Li, V. Chigrinov, and Y. Q. Lu, Opt. Lett. **37,** 3627 (2012).
38. J. Yan, Y. Li, and S. T. Wu, Opt. Lett. **36,** 1404 (2011).
39. G. Zhu, J. N. Li, X. W. Lin, H. F. Wang, W. Hu, Z. G. Zheng, H. Q. Cui, D. Shen, and Y. Q. Lu, J. Soc. Inf. Disp. **20,** 341 (2012).